

A FAST TOPOGRAPHIC MAPPING SYSTEM BASED ON PANORAMIC VISION FOR NEAR REGION TERRAIN CORRECTION IN REGIONAL GRAVITY SURVEY

Kaichang Di^{*1}, Kai Wu², Zhaoqin Liu³, Wenhui Wan⁴, Zhizhong Di⁵, Gang Li⁶

¹Professor, Institute of Remote Sensing Applications, Chinese Academy of Sciences,
P. O. Box 9718, Datun Road, Chaoyang District, Beijing 100101, China; Tel: + 86-010-64868229;
E-mail: kcdi@irsa.ac.cn

²Graduate student, Institute of Remote Sensing Applications, Chinese Academy of Sciences,
P. O. Box 9718, Datun Road, Chaoyang District, Beijing 100101, China; Tel: + 86-010-64807987;
E-mail: wukai@irsa.ac.cn

³Associate Professor, Institute of Remote Sensing Applications, Chinese Academy of Sciences,
P. O. Box 9718, Datun Road, Chaoyang District, Beijing 100101, China; Tel: + 86-010-64807987;
E-mail: liuzq@irsa.ac.cn

⁴Graduate student, Institute of Remote Sensing Applications, Chinese Academy of Sciences,
P. O. Box 9718, Datun Road, Chaoyang District, Beijing 100101, China; Tel: + 86-010-64807987;
E-mail: whwan@irsa.ac.cn

⁵Professor, Beijing Explo-Tech Engineering Co., Ltd.
9 Qinghe Rd., Haidian District, Beijing 100085, China; Tel: +86-010-58584401;
E-mail: dizz@hotmail.com

⁶Engineer, Beijing Explo-Tech Engineering Co., Ltd.
9 Qinghe Rd., Haidian District, Beijing 100085, China; Tel: +86-010-58584401;
E-mail: 50878905@qq.com

KEY WORDS: topographic mapping, regional gravity, panoramic vision, stereo matching, point cloud filtering

ABSTRACT: Corrections for terrain effects is critical in regional gravity survey. The main challenge for gravity correction is how to rapidly reconstruct high-quality terrain relatively close to the gravity survey station. In this research, we design and develop a fast topographic mapping system based on panoramic stereo vision and photogrammetry techniques. The developed software system generates topographic product automatically from panoramic stereo images. The system has been verified in several filed tests with various terrain circumstances. The test results demonstrate that the developed mapping system significantly outperforms the traditional field surveying methods in efficiency and accuracy.

1. INTRODUCTION

In regional gravity survey, topographic correction is necessary to remove the bias in gravity measurements imposed by terrain relief around the gravity survey station (Ketelaar, 1987). Since near region topography affects the gravity measurements more significantly than far zone, the main challenge for gravity correction is how to rapidly reconstruct high-quality terrain relatively close to the gravity survey station, e.g., within a range of 30m. Currently in China's regional gravity survey, the near region terrain correction requires a mapping accuracy of better than 1m and a digital elevation model (DEM) resolution of 1m. According to this requirement, near region DEMs can be obtained from existing large-scale topographic mapping databases. If such databases are not available, the required near region DEMs are usually acquired by digitization of large-scale topographic maps (Ma et al., 2008) or from direct field surveying using total stations, both are time-consuming and laborious.

In this research, we design and develop a fast topographic mapping system for near region terrain correction. The mapping system acquires panoramic stereo images around a gravity station by rotating a stereo camera horizontally and vertically through a rotary stage. The developed software system generates topographic product automatically from these panoramic stereo images based on stereo vision and photogrammetry techniques.

The rest of the paper is organized as follows: Section 2 presents the hardware design and accuracy analysis of the mapping system; Section 3 describes the methods of calibration of stereo cameras; Section 4 describes the technical

*Corresponding author

details of the automated mapping procedure; Section 5 shows the experimental results of typical terrains; Conclusions are given in section 6.

2. HARDWARE DESIGN AND ACCURACY ANALYSIS

2.1 Hardware design of the topographic mapping system

As shown in Figure 1, the hardware of the system includes a pair of CCD cameras for stereo image acquisition, a rotary stage to rotate the cameras, and a tripod for holding the imaging system. The stereo cameras are mounted on the two ends of a camera bar, which is fixed to the two-degree-of-freedom rotary stage. The rotary stage can rotate 360° horizontally and ±32° vertically so that the system acquires panoramic stereo images around a gravity station. A laptop computer is used to control the cameras and the rotary stage. The geometric parameters of the stereo camera system are listed in Table 1.



Figure 1. Hardware of the topographic mapping system.

Table 1. Geometric parameters of the camera system.

Camera Type	MV-VE141SC/SM
Stereo base	50cm
Focal length	12mm
Image dimension	1392 * 1040 pixels
Pixel size	6.45μm * 6.45μm

2.2 Theoretical analysis of mapping accuracy

In order to perform near region terrain correction using the developed topographic mapping system, it is important to analyze the attainable mapping accuracy of the stereo camera system. Actually, the selection of camera and the setting of the baseline (see Table 1) are based on theoretical mapping accuracy analysis. Using the geometric parameters of the stereo camera system, the attainable accuracy is obtained from theoretical derivation (Di and Li 2007; Di and Peng, 2011). Through error propagation, the root mean square error in three directions are represented as

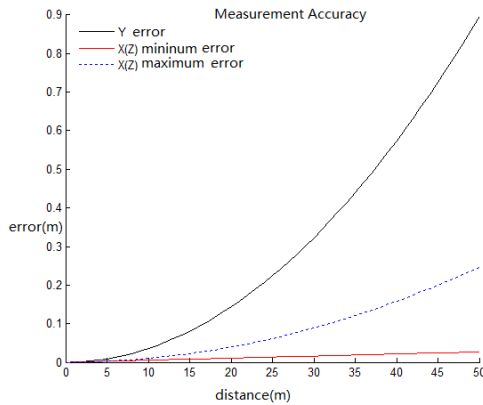


Figure 2. Theoretical mapping accuracy

$$\begin{cases} \sigma_y = \frac{Y^2}{Bf} \sigma_p \\ \sigma_x = \sqrt{\left(\frac{Y^2}{Bf}\right)^2 \left(\frac{x}{f}\right)^2 \sigma_p^2 + \left(\frac{Y}{f}\right)^2 \sigma_x^2} \\ \sigma_z = \sqrt{\left(\frac{Y^2}{Bf}\right)^2 \left(\frac{y}{f}\right)^2 \sigma_p^2 + \left(\frac{Y}{f}\right)^2 \sigma_y^2} \end{cases} \quad (1)$$

where σ_p is the parallax measurement error, which is determined by the accuracy of image matching and is set as 1/3 pixel. Figure 2 shows the standard errors for targets at different distances from the station center. It can be seen that the mapping error in range (Y) direction is larger than that of the other directions. Within 50 meters, the mapping accuracy is better than 1m, which

satisfies the requirements of near region terrain correction.

3. CALIBRATION OF STEREO CAMERAS

It is critical to calibrate the cameras so that to achieve the theoretical mapping accuracy. The task of camera calibration is to determine the interior orientation parameters (focal length, position of principal point) and optical distortion parameters of each camera, and the relative orientation parameters between the two cameras.

Camera calibration is performed at a calibration range where hundreds of precisely measured control points are

evenly distributed in a 3D space (Figure 3). To reduce the time of manual measurement of control points in the images, we developed a semi-automatic method for control point measurement. We only need to manually measure several control points (green crosses in Figure 3), then the rest of control points (red crosses in Figure 3) are extracted automatically by least squares template matching. As we can see, most control points in the image are extracted successfully, which are sufficient for camera calibration. Based on these control points, interior orientation parameters, optical distortion parameters, and exterior orientation parameters are determined through a least squares solution of space resection with collinearity equations. The accuracy of camera calibration is evaluated by the root mean square residual on the control points, which turned out to be 0.15 and 0.174 pixel in column and row directions for the left camera, and 0.158 and 0.167 pixel for the right camera.

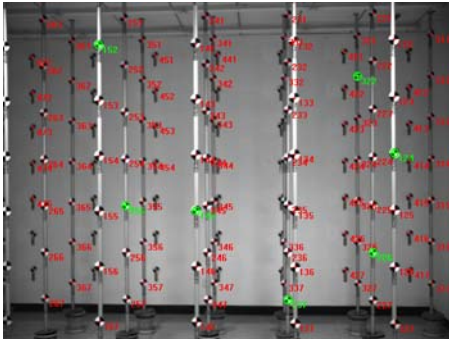


Figure 3. Camera calibration range

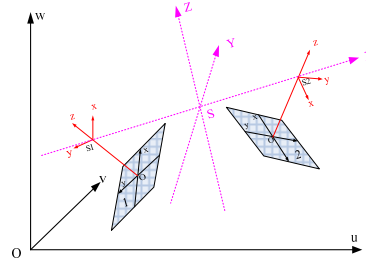


Figure 4. Stereo camera calibration coordinate system

In order to calibrate the relative orientation of the two cameras, a right-handed coordinate system S-XYZ is defined as shown in Figure 4. The line connecting the optical centers of the two cameras is defined as X axis and the center of the line is defined as the origin of the coordinate system. Given the left camera's position vector T_l and orientation matrix R_l , right camera's position vector T_r and orientation matrix R_r , their relation can then be represented as

$$\begin{cases} T_r = -T_l \\ R_r = R_l \cdot R \end{cases} \quad (2)$$

where R is the relative orientation matrix calculated by stereo calibration (Gray et al, 2008).

4. 3D TERRAIN RECONSTRUCTION

After acquisition of panoramic stereo images, the 3D terrain can be reconstructed automatically by the means of batch processing, which largely reduces manual labor. Figure 5 shows the flowchart of 3D terrain reconstruction. The processing steps are as follows. First, radiometric enhancement is conducted by Gaussian filter to remove noises and illumination differences. Second, dense interest points are generated by Förstner operator and matched using normalized correlation coefficients and least squares matching. Matching blunder are detected and removed to improve matching reliability. Third, 3D positions of the matched points are calculated using space intersection with collinearity equations. Fourth, point cloud filtering is employed to remove possible blunders and above-earth objects (e.g., trees). Finally, a DEM is generated using Kriging interpolation from the point cloud.

It's unavoidable that blunder exists in 3D point clouds. A blunder detection algorithm is developed. The steps of this algorithm is as follows: for point P, a window with fixed size centered on P is defined and the median height value is found from the points with the window; if the difference between P's height and the median is above a certain threshold, P is detected as blunder and removed. Furthermore, above-earth points need to be removed in order to reconstruct bare-earth terrain. An adaptive point cloud filtering algorithm (Zhou et al, 2004) is applied for this purpose. The flowchart of the point cloud filtering algorithm is shown in Figure 6.

The 3D points are defined in the leveled local coordinated system (i.e., S-XYZ). In order to get the absolute coordinates in geodetic coordinate system, two ground control points are needed, which can be obtained by GPS.

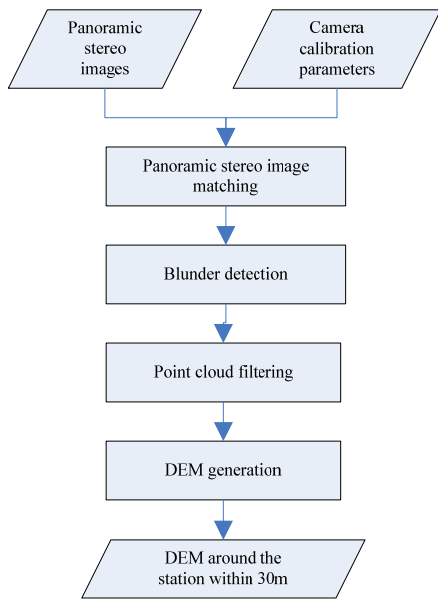


Figure 5. Flowchart of 3D terrain reconstruction.

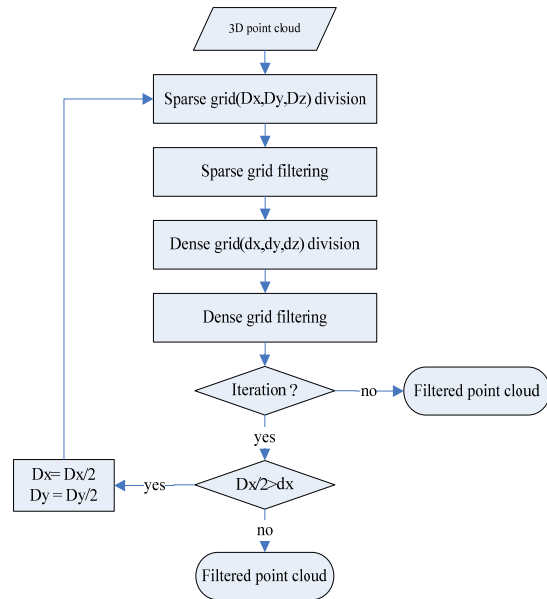


Figure 6. Flowchart of point cloud filtering.

5. EXPERIMENTAL RESULTS

Experiments and field tests have been performed to verify the developed system. In the field test in the area of Ming Tombs in Beijing suburb, panoramic stereo images are collected at 15 stations with various terrain circumstances. Here we report the results of two typical gravity stations. The terrain of Station A is relatively flat; Station B has larger terrain relief and slopes. Panoramic image mosaics (Figures 7 and 8) are generated using an image mosaicking software for better visualization. DEM of the two stations (60m×60m) are automatically generated with a required 1m resolution. Figure 9 shows the DEM of Station A before and after point cloud filtering. Figure 10 shows the DEM of Station B before and after point cloud filtering. It can be seen that point cloud filtering can effectively remove blunders and above-earth points.



Figure 7. Panoramic image mosaic of Station A.



Figure 8. Panoramic image mosaic of Station B.

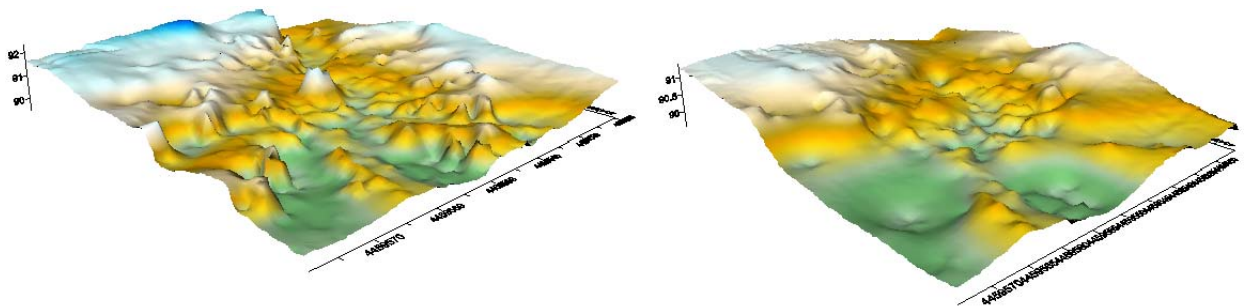


Figure 9. Station A DEM before (top) and after (bottom) and filtering

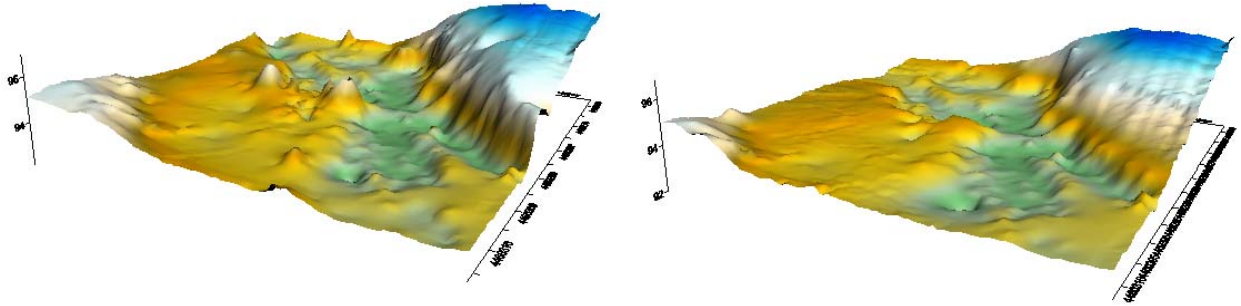


Figure 10. Station B DEM before (top) and after (bottom) and filtering

In our experiments, we evaluate the DEM accuracy using a series of check points (60 for A and 89 for B) evenly distributed in the $60\text{m} \times 60\text{m}$ square areas by comparing the heights at given horizontal positions with their actual height values. Figures 11 and 12 are the height error histograms of the two DEMs. The root mean square errors are 0.46m and 0.84m respectively, which satisfy the required 1m accuracy.

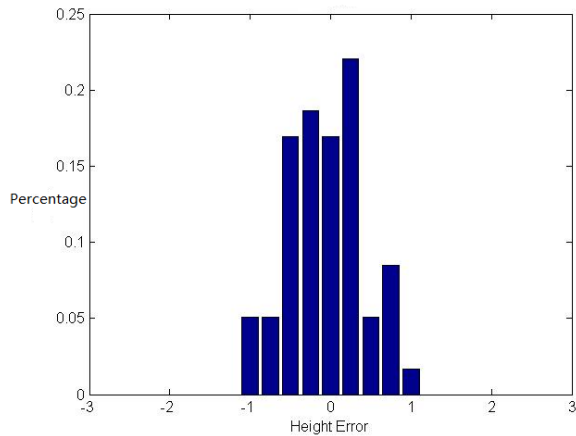


Figure 11. Station A DEM error histogram.

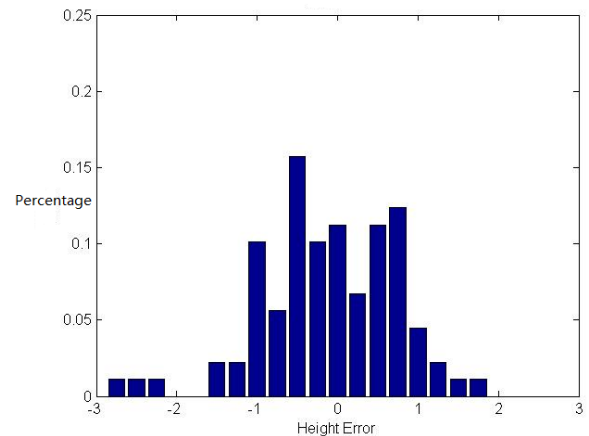


Figure 12. Station B DEM error histogram.

It can be seen from the figures that the error distributions generally satisfy normal distribution. Meanwhile, the height accuracy of the flatter terrain is better than the terrain with larger slopes. This is due to two reasons: occlusions are likely to exist in the images of the terrain with larger slopes which may decrease the final accuracy; horizontal accuracy has a larger effect on height accuracy of the DEM in larger slopes. Overall, the actual mapping accuracy is generally consistent with the theoretical accuracy.

Referring to efficiency, for each station the panoramic image (12 stereo pairs) acquisition time is about 60 seconds and the automatic DEM generation time is about 35 seconds. For most of the test stations, the DEM generation process is fully automatic without human intervention. For some stations where there are dense trees, some manual operation is necessary, which may take several minutes. This is a significant improvement than traditional methods, such as field surveying with total station. Since this mapping system automatically collects much more 3D points of the terrain than field surveying, the overall accuracy of the DEM is also higher.

6. CONCLUSIONS

In this paper, we presented a fast topographic mapping system based on panoramic vision for near region terrain correction in regional gravity survey. The hardware design, system calibration, theoretical accuracy, and the automated DEM generation techniques are described. The experimental results demonstrated that the developed mapping system significantly outperforms the traditional field surveying methods in efficiency and accuracy. The software system will be further enhanced in the future. More field tests will be performed to validate this new mapping system so that it can be applied in practical applications.

Acknowledgement: This research is supported by Beijing Explo-Tech Engineering Co., Ltd.

References

- Di, K., R. Li, 2007. Topographic Mapping Capability Analysis of Mars Exploration Rover 2003 Mission Imagery. 5th International Symposium on Mobile Mapping Technology (MMT 2007), Padua, Italy, May 28-31.
- Di, K, M. Peng, 2011. Wide Baseline Mapping for Mars Rovers. *Photogrammetric Engineering & Remote Sensing*, 77(6), pp. 1-10
- Feng, W., 2002. Close-range Camera Calibration. In: *Close-range Photogrammetry*, edited by Jinlong Wang, Wuhan, pp. 185-215
- Gary, B., and A. Kaebler, 2008. Projection and 3D Vision. In: *Learning OpenCV*, edited by Mike Loukides, USA, pp.405-431.
- Ketelaar, A.C.R., 1987. Terrain Correction for Gravity Measurements Using a Digital Terrain Model. *Geoexploration*, 24, pp. 109-124.
- Li, Z., and Q. Zhu, 2000. *Digital Terrain Model*. Wuhan Technical University of Surveying and Mapping Press, Wuhan, pp.93-101.
- Ma, G., L. Meng, X. Du, 2008 . Gravity of the Terrain in Accomplish by computer. *Journal of Jilin University (Earth Science Edition)*, 38(Sup), pp.36-38.
- Zhou, F., 2004. An Adaptive Point Cloud Filtering Algorithm for DEM Generation from Airborne Lidar Data. National Cheng Kung University, Taiwan, pp.27-42.